Impairment of a model peptide by oxidative stress: Thermodynamic tabilities of asparagine diamide Cα-radical foldamers

Klára Z. Gerlei, Lilla Élő, Béla Fiser, Michael C. Owen, Imre Jákli, Svend J. Knak Jensen, Imre G. Csizmadia, András Perczel, Béla Viskolcz

1. Introduction

Asparagine (Asn) is a non-essential amino acid; its side-chain has a carboxylamide functional group, which is the b-amide derivative of the aspartic acid (Asp). Asn is unstable under physiological conditions and spontaneously, that is non-enzymatically, deamidates into Asp [1,2]. Asparagine plays an important role in the bio-synthesis of glycoproteins [3–5] and is essential to the synthesis of a large number of plant proteins [6]. The active sites of enzymes frequently contain Asn residues [7,8]. The neurotoxin and potential carcinogen acrylamide could be formed in foods by the thermal degradation of free asparagine (roasting, baking or frying at high temperatures) in the presence of sugars [9,10] and also be formed at physiological conditions as a result of asparagine oxidation [11].

Due to these, as well as other biochemical processes [12–17], the asparagine deamidation Asn / Asp is one of the most important protein degradation pathways and residues of Asp serve as 'molecular timers' that can have effects on the protein turnover and aging [18–22]. Some time ago, Clarke et al. proposed not only a mechanism of deamidation, but also claimed that L to D racemization is associated with deamidation in some way [23,24]. More recently, Trout and co-workers [12] and subsequently Catak et al. [25] studied the deamidation process of the Asn at DFT level of theory. However, their study was not extended to L / D racemization. The racemization was subsequently explained by enolization of the H-C-C=O moiety [26], as shown in some details in Scheme S1.

Few calculations have been done on unprotected asparagines [27]. Hydrogen atom abstraction in the gas phase was studied by Galano et al. [28] using B3LYP/6-311G(d, p) calculations. They provided quantitative information about the mechanism and kinetics of the reaction, including the transition states and the temperature dependence of the rate constants. However, they did not study all the possible radical centers. More recently, the α-radical of N-acetyl-asparagine-N-methylamide was investigated in details at the same level of theory [29].

2. Scope

The overall purpose of the present Letter is to study the thermo-dynamics of radical formation which could be a key intermediate for L to D racemization (Scheme 1) and may be related to molecular

aging. Asparagine diamide has been chosen as a model compound, because it has a polar side-chain that could stabilize structures by side-chain-backbone hydrogen bonding. We use DFT methods to study the hydrogen abstraction from an (L)-asparagine residue by an OH radical, both in the gas phase and in solution. N- and C-protecting groups, Ac and NHMe, on Asn made it conformationally and electronically behave like a peptidyl unit. Such a modification with respect to a zwitterion is required to obtain the simplest realistic biomolecular system. The hydroxy radical was chosen as the agent responsible for H(•) abstraction named by their parent heavy atom and are numbered accordingly. For example C3 means that the H3 was abstracted from the alpha carbon atom, Ca or Cα, to which it was attached. Similarly N1 indicates a radical in which H1 is removed from the amide nitrogen atom of the N-terminus of the alpha-L amino acid residue.

3. Theoretical details

This Letter follows the accurate computations of Galano et al. [28] and the more recent computation [29] on asparagine a-radical at the same level as well as at two higher levels of theory. The pres-ent study explores all radical species that can be derived from N-and C-protected Asn. For all the computations the GAUSSIAN09 program package [32] was used. Optimized geometries and energetic of N-and C-pro-tected Asn and its various radicals were calculated by using the density functional theory with the B3LYP functional combined with the 6-31G(d) basis set. All structures were optimized in gas-and aqueous phase (conductor like polarisable continuum model, CPCM was applied). In order to obtain more accurate thermody-namic properties MPWKCIS/6-311++G(3df,2p) single-point ener-gies were also obtained for the B3LYP/6-31G(d) optimized structures. Thermodynamic properties were calculated at $p = 1$ atm and $T = 298.15$ K, using frequencies scaled by 0.97. The
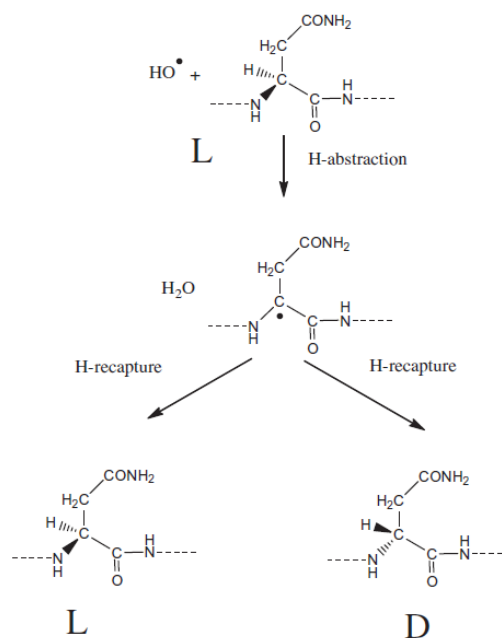
Scheme 1. Proposed free-radical scheme of Asn racemization via free radical attack on the a-CH bond.

as it is by far the most important among the oxidants in cellular systems [30]. The half-life of the hydroxyl radical, OH( ), is about a nanosecond at physiological conditions within a cell [31], which is the shortest half-life among the reactive oxygen species. In our first calculations, the backbone was maintained in an ex-tended bL conformation and the side-chain orientation was arranged to maximize the number of hydrogen bonds between the side-chain and the backbone.

All the C- and N-atoms within Asn could be considered as possible sites for H(•) abstraction (Scheme 2A). All free H radicals are transition states were determined by systematic search. For C3 or Ca-radical the full Ramachandran PES, E = E(φ, Ψ) at x0, x, v1, v2 kept as 180L, was scanned at B3LYP/6-31G(d) basis set with 30L intervals. By interpolation this surface was refined to produce a final 10L virtual resolution. This resulted in a final toroidal surface composed of a total of (36 _ 36) grid-points: DE ¼ f ðu; wÞ. The Ramachandran surface of N- and C protected Asn is shown in Fig-ure S2. The geometries of the extended backbone optimizations are shown in Figure S1 with the associated thermodynamic calcula-tions, reported in Figures 1, S4 and Table 1. The Ramachandran of the C3 or alpha radical's potential energy surface is given in Figure S3.
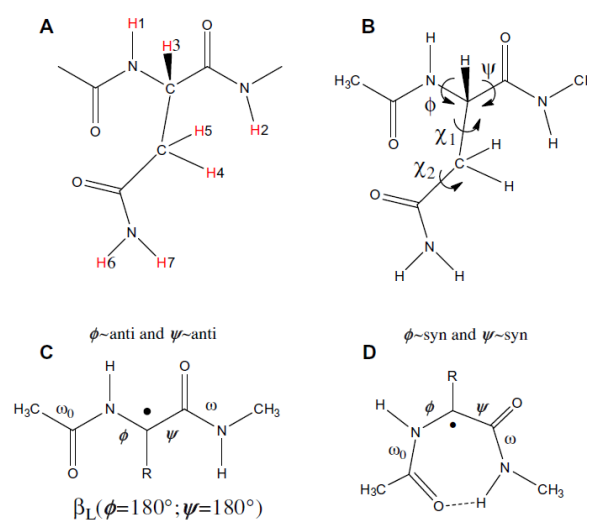
Scheme 2. (A) An Asn residue within a polypeptide chain with all potential H radical forming sites labeled 1–7. (B) The backbone (φ,Ψ) and side-chain (χ_1, χ_2) torsional angles of L-Asn diamide, the first three bonds are linked to Ca of the amino acid residue. (C) Schematic diagram of the fully extended C3 or CA radical. (D) Schematic diagram of the syn-syn conformation of the C3 CA radical.

Table 1   Calculated changes in thermodynamic functions ($\Delta G°$ and $\Delta H°$/kJ/mol) for the various species in (1). The separated reactants (SR) are used as a reference state.

Species	B3LYP/6-31G(d)				MPWKCIS/6-311++G(3df, 2p)//B3LYP/6-31G(d)			
	$\Delta G°$		$\Delta H°$		$\Delta G°$		$\Delta H°$	
	Gas	Aqueous	Gas	Aqueous	Gas	Aqueous	Gas	Aqueous
RC								
C3	7	0	−27	−35	20	13	−14	−22
C4	−12	−5	−49	−44	7	14	−30	−25
C5	−19	−5	−56	−44	−1	14	−38	−25
N1	−9	5	−44	−30	9	24	−27	−12
N2	2	−2	−28	−32	15	10	−15	−20
N6	−9	3	−46	−17	10	21	−27	1
N7	−9	7	−46	−18	10	15	−27	−10
TS								
C3	18	6	−23	−35	42	32	0.63	−9
C4	20.	21	−22	−13	49	40	7.26	6
C5	1	19	−41	−18	31	43	−11	6
N1	27	41	−14	−1	72	88	31	46
N2	42	37	6	0	76	72	41	35
N6	35	46	−4	12	70	76	31	42
N7	34	39	−4	6	70	72	31	39
PC								
C3	−137	−123	−174	−154	−132	−124	−169	−155
C4	−84	−85	−121	−110	−84	−94	−121	−119
C5	−95	−88	−129	−124	−97	−87	−131	−123
N1	−7	31	−43	0	19	−2	−17	−33
N2	−16	−20	−44	−45	−12	−10	−40	−34
N6	7	−4	−26	−32	25	10.	−8	−17
N7	7	4	−26	4	25	11	−8	−14
SP								
C3	−132	−138	−129	−137	−148	−152	−146	−151
C4	−67	−97	−58	−88	−92	−122	−83	−114
C5	−78	−97	−71	−88	−102	−122	−95	−114
N1	−10	−38	−1	−31	−13	−45	−5	−38
N2	−18	−36	−11	−25	−29	−47	−22	−35
N6	−8	−36	1	−8	−14	−23	−5	−15
N7	−2	−17	3	−7	−11	−24	−7	−14

4. Results and discussion

4.1. Ramachandran potential energy surface of asparagine diamid

Asparagine diamide is a multiple rotor with three dihedral angles (φ, Ψ, χ_1) connected to the a-carbon atom (Scheme 2B): All three independent variables, namely φ, Ψ, and χ_1 (Scheme 2B) determine the actual form of the potential energy hypersurface (PEHS) associated E = f(φ, Ψ, χ_1, χ_2). The orientation of the side chain (χ_1, χ_2) will affect the appearance of the 2D Ramachandran hypersurface, however, to simplify its appearance χ_1 and χ_2 were allowed to make the maximal number of H-bonds. This happened at χ_1 ~140° and χ_2 ~+90°. If so, then the Ramachandran-surface will have the shape as shown (Figure S2), where both the Cartesian and the toroidal representations of the 2D-PES of E = f(φ, Ψ) are depicted. These DFT calculations suggest that along the major valley of the 2D-PES, the extended βL conformation is the global minimum. Thus, in our initial study, the various free radicals were all generated from the βL-like conformer, with an 'all-anti' (φ = 180° and Ψ = 180°) backbone orientation (Scheme 2C).The comprehensive analysis of the gas phase and aqueous solution PESs suggests that the effect of the continuum solvent model on structure stability is minor if not negligible on the over appearance, even if the aqueous PES appears slightly more flat.
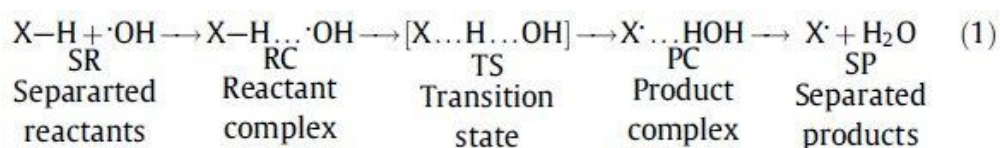
4.2. Molecular structure of βL-asparagine and its radicals

Seven different hydrogen atoms, labeled from H1 to H7 (Scheme 2A) were removed from the parent molecules to generate seven different radicals; all the optimized molecular structures of the parent Asn model and its derived radicals (C3, C4, C5, etc.) were obtained (Figure S1) both in the gas phase and in solution. Among the optimized geometries several hydrogen bonded ring structures were

found. In total three different types of H-bonded structures were recognized, namely those of 5-, 7-, and 8-membered rings. The 7-membered ring structures, with H-bond between the side-chain C=O and the N–H of the N-methyl amide (of the C-terminus) was always present with the exception of the N2 radical. In contrast to the above, an 8-membered ring with a relatively long (2.05 Å) C=O----H–N linkage was found only for C3. This interaction took place between the N-acetyl C=O and of the H–N of side-chain terminal amide group. It has been noticed previously, that the strength of the H-bond is related to the length of the H-bond. [33–34].

4.3. Energetics of radical formation mechanisms

The H-atom abstraction by the OH radical is envisaged to pro-ceed according to a mechanism with four steps:

$$X-H + \cdot OH \longrightarrow X-H \ldots \cdot OH \longrightarrow [X \ldots H \ldots OH] \longrightarrow X^{\cdot} \ldots HOH \longrightarrow X^{\cdot} + H_2O \quad (1)$$

SR	RC	TS	PC	SP
Separarted reactants	Reactant complex	Transition state	Product complex	Separated products

The thermodynamic functions for the four reactions are collected in Table 1. The computed thermodynamic functions along with dihedral angles are listed in Table S1. The variation of DGL along the reaction coordinate of the H-abstraction reaction is shown in the reaction profile (Figure 1), both for the gas phase (top) and for the aqueous phase (bottom). It appears that the reac-tion profiles are quite similar in nature

The overall free energy changes from separated reactants (SR) to separated products (SP) show that the thermodynamically most probable abstraction site is C3 (CA) and C4 (CB) or C5 (CB) is the next most probable site in solution. However, in the gas phase, the reactivity of CB hydrogen atoms is competing with CA. In general, hydrogen abstractions from the N atoms are the thermodynamically least favored and the associated activation energies are higher. This observation applies for both the gas- and aqueous phase for both levels of calculations.

4.4. Potential energy surface of the N- and C-protected-Asn C3 or CA-radical

In the βL and βD conformation, the radical center is close to planar. For the γL and γD radicals the α-carbon atom is nearly planar (sum of the three bond angles is 357L). Yet βL and βD as well as the γL and γD conformations have identical energies because they are enantiomers. This implies that the chirality was induced by non-symmetric side-chain orientations. This is clearly seen in Figure 2 from the non-superimposable mirror image structures. Such axis chirality has recently been studied theoretically in a general case [35]. Following some earlier studies [36,37] the Ramachandran-surface of the a-radical (C3) was computed [38]. Figure S3 shows both the Cartesian as well as the toroidal [39] representations of Ramachandran type Potential Energy Surfaces (PES), where two low energy regions are recognized.
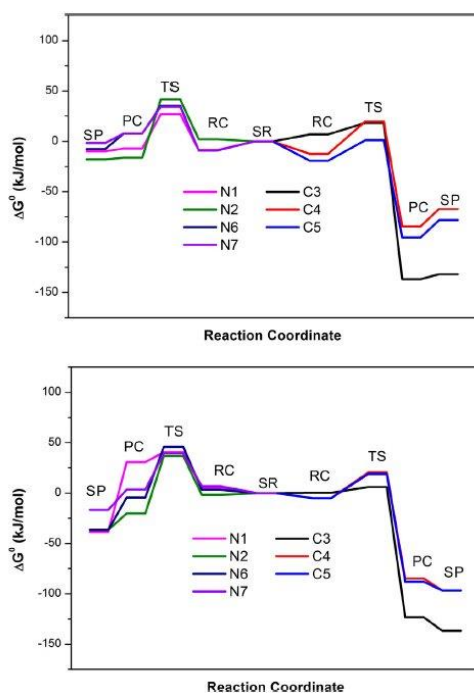
Figure 1. Standard free energy change (DGL) associated with the mechanism in (1) for (L)-Asn diamide and OH in gas phase (top) and in aqueous phase (bottom). All reactions pertaining to the seven radical centers (C3, C4, etc.) are color coded. The reaction starts at the center specified as SR (Separated reactant). Reactions to the right are for C–H abstractions while reactions to the left are for the N–H abstraction. The SR state is taken to be reference state for the calculation of DGL.
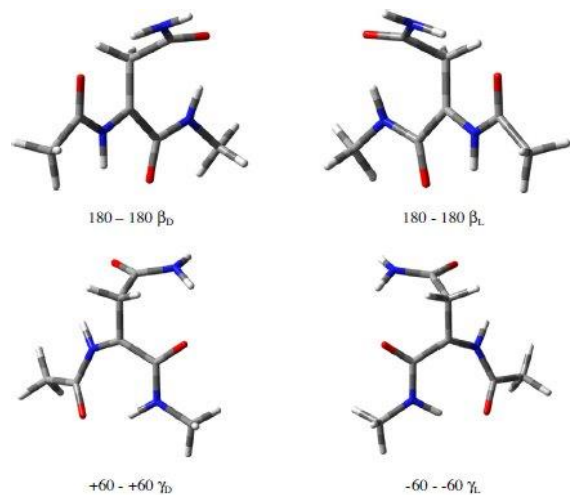

Figure 2. Non-superimposable mirror image structures of extended βL and βD as well as γL and γD Asn α-radicals.

One is a β type or the extended backbone conformer (Scheme 2C), close to an anti-anti orientation ($\varphi \sim \Psi \sim 180°$). Another type of foldamer region is something like structure, close to ($\varphi \sim \Psi \sim 0°$ Scheme 2D), that is a syn–syn arrangement. Geometry search in these two regions revealed a clear βL and βD conformations in the former case and two closely spaced conformations corresponding to γL and γD in the latter case. A pair of highest energy minima were also located which corresponded to the εL and εD foldamers. The geometrical parameters of these conformers are summarized in

Table 2. Search for additional minima on the radical potential energy surface revealed relatively high energy minima for εL and εD.

Species	B3LYP/6-31G(d)				MPWKCIS/6-311++G(3df, 2p)//B3LYP/6-31G(d)			
	DGL		DHL		DGL		DHL	
	Gas	Aqueous	Gas	Aqueous	Gas	Aqueous	Gas	Aqueous
RC								
C3	7	0	_27	_35	20	13	_14	_22
C4	_12	_5	_49	_44	7	14	_30	_25
C5	_19	_5	_56	_44	_1	14	_38	_25
N1	_9	5	_44	_30	9	24	_27	_12
N2	2	_2	_28	_32	15	10	_15	_20
N6	_9	3	_46	_17	10	21	_27	1
N7	_9	7	_46	_18	10	15	_27	_10
TS								
C3	18	6	_23	_35	42	32	0.63	_9
C4	20.	21	_22	_13	49	40	7.26	6
C5	1	19	_41	_18	31	43	_11	6
N1	27	41	_14	_1	72	88	31	46
N2	42	37	6	0	76	72	41	35
N6	35	46	_4	12	70	76	31	42
N7	34	39	_4	6	70	72	31	39
PC								
C3	_137	_123	_174	_154	_132	_124	_169	_155
C4	_84	_85	_121	_110	_84	_94	_121	_119
C5	_95	_88	_129	_124	_97	_87	_131	_123
N1	_7	31	_43	0	19	_2	_17	_33
N2	_16	_20	_44	_45	_12	_10	_40	_34
N6	7	_4	_26	_32	25	10.	_8	_17
N7	7	4	_26	4	25	11	_8	_14
SP								
C3	_132	_138	_129	_137	_148	_152	_146	_151
C4	_67	_97	_58	_88	_92	_122	_83	_114
C5	_78	_97	_71	_88	_102	_122	_95	_114
N1	_10	_38	_1	_31	_13	_45	5	_38
N2	_18	_36	_11	_25	_29	_47	_22	_35
N6	_8	_36	1	_8	_14	_23	_5	_15
N7	_2	_17	3	_7	_11	_24	_7	_14

5. Conclusions

In agreement with the work of Easton and co-workers [40], the present study has been carried out on an (L)-Asn diamide model system with an anti-anti or extended-like backbone conformation. The side-chain orientation was characterized by a χ_1 equal g$^+$ conformation. In total seven different radicals obtained by H-abstractions were studied, both in the gas phase and in aqueous solution.

The Ramachandran energetic patterns for the gas- and aqueous phase were found to be quite similar. The hydrogen abstraction by OH radical from the CH bonds was thermodynamically more favored than the hydrogen abstraction from NH bonds. The C3 or Cα radical was thermodynamically more stable than the radical generated from the beta carbon. The cylindrical and toroidal representation of the alpha radical revealed that not only the anti-anti or extended backbone conformation, but also syn–syn or inverse c-turns have a substantial stability too.

References

[1]   A.B. Robinson, C.J. Rudd, Curr. Top. Cell. Regul. 8 (1974) 247.

[2]   P. Bornstein, G. Balian, J. Biol. Chem. 245 (18) (1970) 4854.

[3]   S.E. O'Connor, B. Imperiali, J. Am. Chem. Soc. 119 (9) (1997) 2295.

[4]   B. Imperiali, K. Shannon, K. Rickert, J. Am. Chem. Soc. 114 (20) (1992) 7942.

[5]   B. Imperiali, Acc. Chem. Res. 30 (11) (1997) 452.

[6]   P.J. Lea, L. Sodek, M.A.J. Parry, P.R. Shewry, N.G. Halford, Ann. Appl. Biol. 150 (1) (2007) 1.

[7]   J. Mansfeld, S. Gebauer, K. Dathe, R. Ulbrich-Hofmann, Biochemistry 45 (18) (2006) 5687.

[8]   F. Himo, Theor. Chem. Acc. 116 (1–3) (2005) 232.

[9]   D.V. Zyzak et al., J. Agric. Food Chem. 51 (16) (2003) 4782.

[10] R.H. Stadler et al., Nature 419 (6906) (2002) 449. [11]   E. Tareke, T.M. Heinze, G. Gamboa da Costa, S. Ali, J. Agric. Food Chem. 57 (20) (2009) 9730.

[12]   B. Peters, B.L. Trout, Biochemistry 45 (16) (2006) 5384.

[13]   N. Robinson, A. Robinson, J. Pept. Res. 63 (5) (2004) 437.

[14]   N. Robinson, Z. Robinson, B. Robinson, A. Robinson, J. Robinson, M. Robinson, A. Robinson, J. Pept. Res. 63 (5) (2004) 426.

[15]   J. Radkiewicz, H. Zipse, S. Clarke, K. Houk, J. Am. Chem. Soc. 123 (15) (2001) 3499.

[16]   F.A.S. Konuklar, V. Aviyente, Org. Biomol. Chem. 1 (13) (2003) 2290.

[17]   A.L. Heaton, P.B. Armentrout, J. Am. Soc. Mass Spectrom. 20 (5) (2009) 852.

[18]   S.J. Weintraub, S.R. Manson, Mech. Ageing Dev. 125 (4) (2004) 255.

[19]   N.E. Robinson, A.B. Robinson, Proc. Natl. Acad. Sci. USA 98 (3) (2001) 944.

[20]   S. Ritz-Timme, I. Laumeier, M. Collins, Int. J. Legal Med. 117 (2) (2003) 96.

[21]   S. Ohtani, T. Yamamoto, J. Forensic Sci. 55 (6) (2010) 1630.

[22]   C.T. Thorpe, I. Streeter, G.L. Pinchbeck, A.E. Goodship, P.D. Clegg, H.L. Birch, J. Biol. Chem. 285 (21) (2010) 15674.

[23]   S. Clarke, Int. J. Pept. Protein Res. 30 (6) (1987) 808.

[24]   T. Geiger, S. Clarke, J. Biol. Chem. 15 (262) (1987) 785.

[25]   S. Catak, G. Monard, V. Aviyente, M.F. Ruiz-López, J. Phys. Chem. A 112 (37) (2008) 8752.

[26]   N. Fujii, S. Tajima, N. Tanaka, N. Fujimoto, T. Takata, T. Shimo-oka, Biochem. Biophys. Res. Commun. 294 (2002) 1047.

[27]   W.D. Arnold et al., J. Am. Chem. Soc. 122 (19) (2000) 4708.

[28]   A. Galano, J. Alvarez-Idaboy, G. Bravo-Pérez, M.E. Ruiz-Santoyo, J. Mol. Struct. 617 (1–3) (2002) 77.

[29]   K.Z. Gerlei, I. Jákli, M. Szori,} S. Knak Jensen, B. Viskolcz, I.G Csizmadia, A. Perzel, J. Phys. Chem. B 117 (41) (2012) 12402.

[30]   H.M. Hassan, L.B. Clerch, D.J. Massaro, Oxygen, Gene Expression and Cellular Function, Marcel Dekker, New York, 1997.

[31]   R.J. Reiter, D. Tan, C. Osuna, E. Gitto, J. Biomed. Sci. 7 (2000) 444.

[32]   M.J. Frisch et al., GAUSSIAN 09, Revision A.02, Gaussian Inc, Wallingford, CT, USA, 2009.

[33]   I.Y. Torshin, I.T. Weber, R.W. Harrison, Protein Eng. 15 (5) (2002) 359.

[34]   T.-H. Tang, E. Deretey, S. Knak Jensen, I.G. Csizmadia, Eur. Phys. J. D 37 (2006) 217.

[35]   T.-H. Tang, M. Nowakowska, J.E. Guillet, I.G. Csizmadia, J. Mol. Struct. 232 (1991) 133.

[36]   M.C. Owen, B. Viskolcz, I.G. Csizmadia, J. Chem. Phys. 135 (3) (2011) 035101.

[37]   M.C. Owen, B. Viskolcz, I.G. Csizmadia, J. Phys. Chem. B 115 (2011) 8014.

[38]   M.C. Owen, M. Szori, I.G. Csizmadia, B. Viskolcz, J. Phys. Chem. B 116 (3) (2012) 1143.

[39]   I. Jákli, S. Knak Jensen, I.G. Csizmadia, Chem. Phys. Lett. 547 (2012) 82.

[40]   B. Chan, R.J. O'Reilly, C.J. Easton, L. Radom, J. Org. Chem. 77 (21) (2012) 9807.